

Theoretical Investigation of the Excited States of Coumarin Dyes for Dye-Sensitized Solar Cells

Yuki Kurashige,* Takahito Nakajima, Saki Kurashige, and Kimihiko Hirao

Department of Applied Chemistry, School of Engineering, The University of Tokyo, Tokyo 113-8656, Japan

Yoshinori Nishikitani

Central Technical Research Laboratory, Nippon Oil Corporation, Yokohama, Kanagawa 231-0815, Japan

Received: March 14, 2007; In Final Form: April 24, 2007

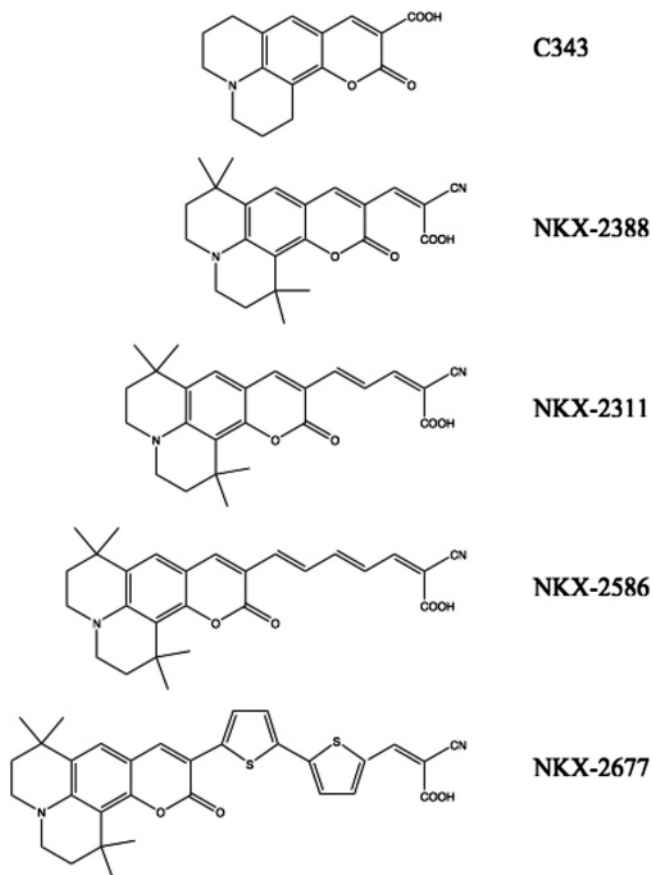
Using time-dependent density functional theory (TD-DFT), configuration interaction single (CIS) method, and approximate coupled cluster singles and doubles (CC2) method, we investigated the absorption spectra of coumarin derivative dyes (C343, NKX-2388, NKX-2311, NKX-2586, and NKX-2677), which have been synthesized for efficient dye-sensitized solar cells. The CC2 calculations are found in good agreement with the experimental results except for the smallest coumarin dye (C343). TD-DFT underestimates the vertical excitation energy of the larger coumarin dyes (NKX-2586 and -2677). Solvents (methanol) are found to induce a red shift of the vertical excitation energies, and their effects on the molecular geometry and the electronic structure are examined in detail. The deprotonated form of coumarin is also investigated, where a blue shift of the vertical excitation energies is observed.

I. Introduction

Dye-sensitized solar cells (DSSC) have been vigorously studied as an alternative to the solid-state photovoltaic cells since Grätzel et al. reported high conversion efficiency using a Ru complex photosensitizer.¹ Organic dyes, which are available at a low cost, have also been actively studied due to their large absorption coefficients in the π - π^* transitions. In DSSCs, the dye is present as a monolayer at the interface between a wide band gap semiconductor electrode such as TiO₂ and ZnO and a redox electrolyte such as I⁻/I₃⁻. The DSSC process is initiated by absorption of photons by the dye. The electronic excitation induces a quick injection of the electrons into the semiconductor electrode. The oxidized dye then accepts an electron from the I⁻ redox mediator and further oxidizes the I⁻ to I₃⁻. In this process, the conversion efficiency of DSSC is primarily determined by the electron transportation ability and the absorption spectra in the visible region of the dye, i.e.: (1) To accept electrons from the electrode, the energy level of the highest occupied molecular orbital (HOMO) of the dye must be higher than the redox potential. (2) To inject electrons into the electrolyte, the energy level of the lowest unoccupied molecular orbital (LUMO) of the dye must be higher than the conduction band of the semiconductor. (3) To obtain an efficient charge separation, the excited states must have a charge-transfer nature from the electrode side to the electrolyte side. (4) To absorb more photons from the sun, the dye must have broad absorption spectra in the visible region.

In this paper, we study the molecular structure and the electronic properties of the ground and lowest π - π^* excited state for a series of coumarin derivatives, C343, NKX-2388, NKX-2311, NKX-2586, and NKX-2677 (Scheme 1), with and without the solvent effects. The series of NKX-xxxx series of molecules, recently synthesized by Hara et al.,²⁻⁴ have been reported as useful candidates for organic dyes for an efficient DSSC. NKX-2677, for example, has shown the highest conver-

SCHEME 1: Molecular Structures of C343, NKX-2388, NKX-2311, NKX-2586, and NKX-2677



sion efficiency (7.4%) among the other organic dye photosensitizers. It is notable that this conversion efficiency is comparable

to the conversion efficiency of the DSSCs based on Ru complex photosensitizers.^{5–7}

Despite the intensive industrial interest in these coumarin derivatives, to our best knowledge, theoretical studies still remain rather few. There have been theoretical reports on relatively smaller coumarins.^{8–16} These studies showed that TD-DFT¹⁷ reproduces the experimental electronic transitions independently of the chemical environment and substitutions of the coumarin. Moreover, statistical corrections based on a linear regression improved the agreement^{11,14} with the experimental values. Moreover, these studies indicate that the vibronic,^{12,13} basis sets, and state-specific treatment of solvent effect¹⁵ could also be significant, which is not addressed here. In this study, we employ the CC2 method,¹⁸ which is a reliable approach to incorporate the electron correlation effects,^{19,20} and compare the CC2 results with the TD-DFT results. The reliability of TD-DFT for treating coumarin dyes is discussed. Furthermore, the chemical environments and substitution effect on the excitation properties of the coumarin dyes are investigated, which is essential for designing highly efficient solar cells.

II. Computational Details

We have considered three different chemical environments to analyze the solvent and deprotonation ($-\text{COOH}$ to $-\text{COO}^-$) effects in the coumarin dyes: (1) the $-\text{COOH}$ form in the gas phase, (2) the $-\text{COOH}$ form in methanol solution, and (3) the $-\text{COO}^-$ form in methanol solution ($-\text{COOH}$ and $-\text{COO}^-$ denote the carboxyl and carboxyl-anion group, respectively). Solvent effects were included by the polarizable continuum model (PCM).²¹

Geometry optimizations of the coumarin dyes (Scheme 1) in the ground state have been performed at the B3LYP/6-31G(d,p) level. Vibrational frequency calculations also have been performed to confirm the stability of the optimized geometries. The vertical excitation energies and oscillator strengths were calculated at these geometries in each chemical environment using TD-DFT with the 6-31+G(d,p) basis set,^{22–25} the CIS with the 6-31+G(d,p) basis set, and the CC2 with the SV(P)²⁶ basis set. The oscillator strengths were calculated by the dipole approximation. The resolution of the identity approximation was used in the CC2 calculations (RI-CC2).²⁷ Solvent effects were taken into account by the PCM of nonequilibrium solutions²⁸ in the CIS and TD-DFT calculations. The CC2 excitation energies in solution were estimated by adding the difference between the CIS and PCM-CIS excitation energies.

The geometry optimizations, the TD-DFT and the CIS calculations were all performed with the GAUSSIAN03 suite of programs.²⁹ The CC2 calculations were performed with the TURBOMOLE program package.³⁰ Unless otherwise stated, the default settings have been used (for example, the pruned grids for DFT, thresholds for convergence of the geometry optimizations and the self-consistent fields).

III. Results and Discussion

A. Ground-State Optimized Geometries. For each coumarin dye, the optimized geometries are found to be nearly planar and syn conformation with respect to the nitrogen atom of the unsaturated rings. For NKX-2388, -2311, and -2586 coumarin dyes, two different stable structures are located, namely, cis and trans isomers at the single bond (s-cis and s-trans isomers) between the coumarin moiety and the methine group. Table 1 shows the relative energies of the two isomers at the B3LYP/6-31G(d,p) level for NKX-2388, -2311, and -2586 coumarin dyes. For NKX-2311 and -2586 coumarin dyes, the relative

TABLE 1: Relative Energies of s-Cis and s-Trans Isomer of NKX-2388, -2311, and -2586 Coumarin Dyes (kcal/mol)

	gas phase	methanol solution	
	$-\text{COOH}$	$-\text{COOH}$	$-\text{COO}^-$
NKX-2388			
s-cis	0	0	0
s-trans	6.3	2.4	2.9
NKX-2311			
s-cis	0	0.7	0.6
s-trans	0.3	0	0
NKX-2586			
s-cis	0.8	0.6	0.5
s-trans	0	0	0

energies of the two isomers are very small, within 0.8 kcal/mol. For NKX-2388 coumarin dye, however, the s-cis isomers are more stable than the s-trans isomers by 6.3, 2.4, and 2.9 kcal/mol for the $-\text{COOH}$ form in the gas phase, the $-\text{COOH}$ form in methanol, and the $-\text{COO}^-$ form in methanol, respectively.

The zero-point energies of the NKX-2311 coumarin dye are obtained as 293.02, 291.19, and 283.81 kcal/mol for the s-cis isomer and 293.01, 291.23, and 283.87 kcal/mol for the s-trans isomer for the $-\text{COOH}$ form in the gas phase, the $-\text{COOH}$ form in methanol solution, and the $-\text{COO}^-$ form in methanol solution, respectively. Because the zero-point energies of the two isomers are virtually equal, the zero-point correction does not alter the relative energies of the two isomers.

In the previous study,² the s-cis isomer has been suggested to be more stable than the s-trans isomer due to the steric repulsion between the oxygen atom of the $\text{C}=\text{O}$ group in the coumarin moiety and the nitrogen atom of the $-\text{C}\equiv\text{N}$ group. The present result supports this suggestion for NKX-2388. It is interesting, however, that the steric repulsion seems unimportant for the larger coumarin dyes with a longer polymethine chain.

Figure 1 shows the optimized geometries of the s-cis and s-trans isomers of the NKX-2311 coumarin dye in each chemical environment. The solvent effect is found to reduce the bond alternation of the π -conjugated chain including the $-\text{C}-\text{O}-\text{C}=\text{O}$ group in the coumarin moiety. The maximum change in the $\text{C}-\text{C}$ bond lengths is 0.010 Å for 11C–12C in both the s-cis and s-trans isomers. The 16N–15C bond becomes shorter by 0.013 Å. The deprotonated form ($-\text{COO}^-$) is found to induce the bond alternation of π -conjugated chain, but the $-\text{C}-\text{O}-\text{C}=\text{O}$ group in the coumarin moiety remains virtually unchanged. The maximum change in the $\text{C}-\text{C}$ bond lengths is 0.016 Å for 11C–12C in both the s-cis and s-trans isomers except for the carboxyl-anion ($-\text{COO}^-$) group, which of course drastically changes due to the deprotonation. The 16N–15C bond becomes longer by 0.008 Å. The effect of the geometry relaxation on the vertical excitation energies will be discussed later.

B. Vertical Excitation Energies. To analyze the absorption bands of the coumarin dyes, we investigate the optically active excited states in the visible band. Table 2 shows the vertical excitation energies and the oscillator strengths of the $\pi-\pi^*$ states in each chemical environment at the ground-state geometries together with the experimental results^{2,3} for comparison.

First, we discuss the comparison of the CC2, CIS, and TD-DFT method in calculating the excited state of these coumarin dyes (in the gas phase). All methods reproduce the fact that, the longer π conjugated chain has, the lower the vertical excitation energies. This tendency is in accord with the experimental absorption peaks (λ_{max}) in methanol solution. In addition, the vertical excitation energies and oscillator strengths of the s-cis isomers are always smaller than the s-trans isomers

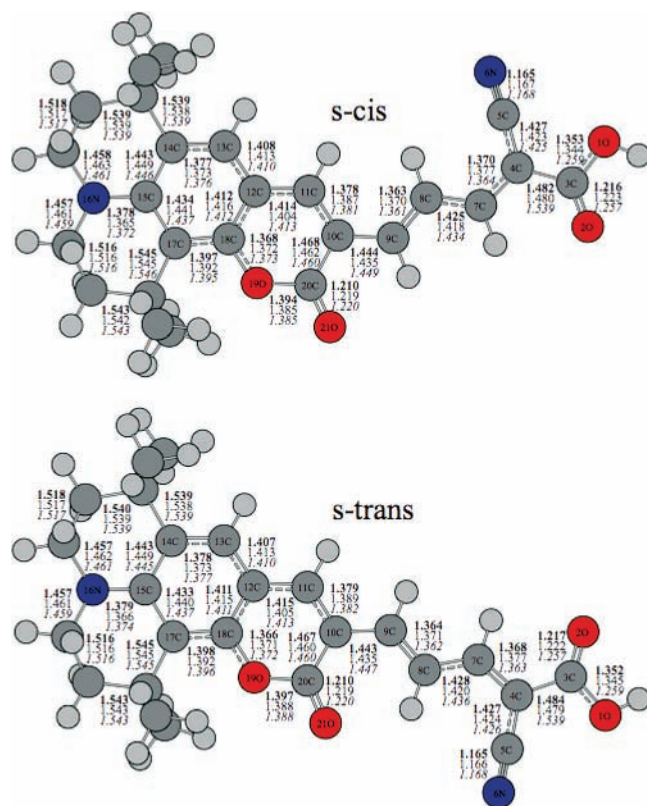


Figure 1. Optimized geometries of the s-cis and s-trans isomers of the NKX-2311 coumarin dye with atom numbering and selected optimized bond lengths of the $-\text{COOH}$ form in the gas phase (**bold**), of the $-\text{COOH}$ form in methanol solution (normal), and the $-\text{COO}^-$ form in methanol solution (*italic*) at the (PCM)-B3LYP/6-31G(d,p) level.

in each method. However, the CIS always overestimates the vertical excitation energies and the oscillator strengths due to the lack of electronic correlation. The CC2 calculations are found in good agreement with the experimental results except for C343, and the TD-DFT underestimates the vertical excitation energies and oscillator strengths for the larger coumarin dyes, i.e., NKX-2586, and -2677, in comparison with the experimental

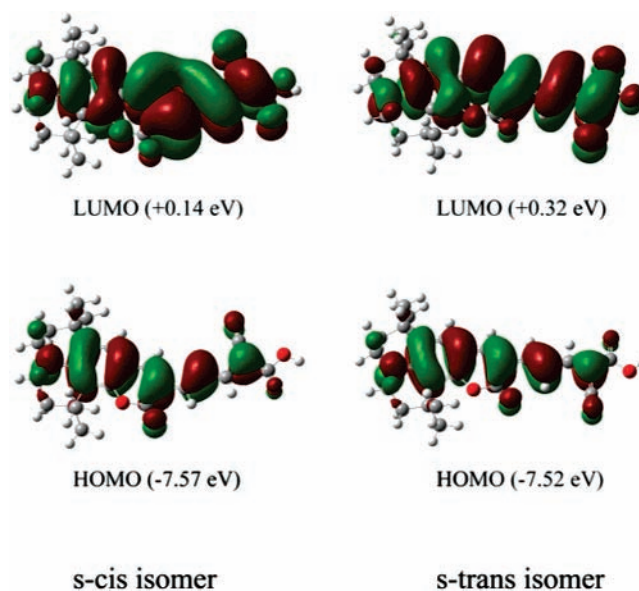


Figure 2. HOMO (π orbital) and LUMO (π^* orbital) of the s-cis and s-trans isomers of the NKX-2311 coumarin dye.

results. We summarize that the CIS calculations are only qualitative, TD-DFT calculations are quantitative except for larger coumarin dyes, and the CC2 method should be used for larger coumarin dyes to obtain quantitative results. Note that there are relatively large discrepancies between the gas-phase calculations and experimental measurements because of the lack of solvent effects in the calculations.

It is interesting that the s-cis and s-trans isomers have different vertical excitation energies, whereas their ground-state energies are very close. The vertical excitation energies of the s-cis isomers are lower than the s-trans isomers by 0.15–0.25, 0.19–0.23, and 0.10–0.13 eV in the CC2, CIS, and TD-DFT calculations, respectively. Figure 2 shows the HOMO and LUMO, and their energy levels for the NKX-2311 coumarin dye in the s-cis and s-trans isomers. On the one hand, the HOMO has a similar nodal structure. On the other hand, the LUMO apparently has a different nodal structure; i.e., the LUMO of s-cis isomer has fewer nodes than that of s-trans isomer, thereby

TABLE 2: Vertical Excitation Energies and Oscillator Strength of π - π^* Excited State of Coumarin Dyes

	gas phase $-\text{COOH}$			methanol						
				$-\text{COOH}$			$-\text{COO}^-$			
	CC2	CIS	B3LYP	CC2 ^a	CIS	B3LYP	CC2 ^a	CIS	B3LYP	exp ^b
Vertical Excitation Energy (eV)										
C343	3.44	4.40	3.32	3.19	4.15	3.09	3.40	4.36	3.23	2.81
NKX-2388 (s-trans)	2.99	3.94	2.90	2.77	3.72	2.70	2.98	3.93	2.86	2.51
(s-cis)	2.80	3.75	2.78	2.56	3.51	2.58	2.73	3.68	2.70	
NKX-2311 (s-trans)	2.89	3.73	2.70	2.63	3.47	2.43	2.86	3.69	2.64	2.46, 2.45
(s-cis)	2.71	3.50	2.56	2.49	3.28	2.34	2.68	3.47	2.51	
NKX-2586 (s-trans)	2.81	3.53	2.50	2.52	3.24	2.21	2.77	3.49	2.44	2.45
(s-cis)	2.66	3.34	2.40	2.41	3.09	2.15	2.62	3.31	2.34	
NKX-2677	2.71	3.12	2.23	2.51	2.92	1.93	2.71	3.12	2.19	2.43
Oscillator Strength (au)										
C343	0.738	0.941	0.603		1.135	0.762		0.961	0.619	15.1 ^c
NKX-2388 (s-trans)	1.064	1.446	0.937		1.646	1.170		1.497	1.033	44.2 ^c
(s-cis)	1.004	1.238	0.867		1.430	1.082		1.279	0.947	
NKX-2311 (s-trans)	1.511	2.113	1.354		2.210	1.545		2.151	1.492	51.9 ^c
(s-cis)	1.329	1.615	1.188		1.720	1.433		1.632	1.296	
NKX-2586 (s-trans)	2.007	2.751	1.709		2.751	1.884		2.768	1.903	59.1 ^c
(s-cis)	1.740	2.129	1.547		2.245	1.780		2.089	1.675	
NKX-2677	2.174	2.184	1.489		2.236	1.436		2.201	1.651	64.3 ^c

^a The CC2 excitation energies in solution were estimated by adding the difference between the CIS and PCM-CIS excitation energies ^b Absorption spectra in methanol solution (normal)² and in *tert*-butyl alcohol–acetonitrile (*italic*).^{3,4} ^c Units of $[\text{mol}/(\text{L}\cdot\text{cm})]^{-1}$.

becoming more stable. Thus, the red shift in going from the s-trans isomer to the s-cis isomer is due to the stabilization of the LUMO (π^* orbital).

Next, we discuss the solvent effect on the vertical excitation energies of the $-\text{COOH}$ form. The vertical excitation energies of the $-\text{COOH}$ form in methanol solution are smaller than in the gas phase by 0.20–0.29 and 0.20–0.30 eV in the CIS and TD-DFT calculations, respectively. This shift can be divided into two contributions, namely, geometry relaxation and solvent polarization effects. The effect of geometry relaxation is evaluated by comparing the vertical excitation energies at the ground-state geometries optimized in the gas phase and in solution, and the effect of solvent polarization is evaluated by comparing the vertical excitation energy in the gas phase and solution at the same geometry optimized in solution. It is observed that the geometry relaxation has a small contribution, in which the vertical excitation energies of the $\pi-\pi^*$ state are reduced only 0.06–0.12 and 0.00–0.02 eV in the CIS and TD-DFT calculations, respectively. In contrast, it is found that the solvent polarization reduces the vertical excitation energies a notable amount by 0.11–0.31 and 0.20–0.26 eV in the CIS and TD-DFT calculations, respectively. Because the $\pi-\pi^*$ state has a charge-transfer nature and is more polarized than the ground state, the excited state is more stabilized than the ground state in solution. Therefore, we conclude that the red shift in solution is mainly caused by the polarization of the solvent. In the previous studies, the red shift in solution has not been observed for a unsubstituted coumarin¹¹ but has been observed for some substituted coumarins.¹⁶

The vertical excitation energies in solution are in much better agreement with the experimental measurements than those in the gas phase. The deviations of the solvent-shifted CC2 energies of the $-\text{COOH}$ form from the experimental values are 0.39 (C343), 0.04, 0.26 (s-cis and s-trans of NKX-2388), 0.03, 0.17 (s-cis and s-trans of NKX-2311), -0.04 , 0.07 (s-cis and s-trans of NKX-2586), and 0.09 (NKX-2677) eV. The deviations in the TD-DFT calculations are 0.28 (C343), 0.06, 0.18 (s-cis and s-trans of NKX-2388), -0.12 , -0.03 (s-cis and s-trans of NKX-2311), -0.30 , -0.24 (s-cis and s-trans of NKX-2586), and -0.50 (NKX-2677) eV. Note that the -0.50 eV error for the NKX-2677 coumarin dye is particularly larger than the others.

Last, we discuss the effect of deprotonation in going from the $-\text{COOH}$ to the $-\text{COO}^-$ form. The previous experimental study² suggested that the coumarin dyes exist in the $-\text{COOH}$ form in methanol solution, but in the $-\text{COO}^-$ form on the TiO_2 surface. In methanol solution, the vertical excitation energies of the $-\text{COO}^-$ form are higher than those of the $-\text{COOH}$ form by 0.17–0.25 and 0.12–0.27 eV in the CIS and TD-DFT calculation, respectively. The blue shift in the $-\text{COO}^-$ form is mainly caused by the unstabilization of the LUMO (π^* orbital) relative to the HOMO (π orbital). The energy levels of the HOMO and LUMO become higher by 0.10–0.25 and 0.42–0.53 eV, respectively. The blue shift in the deprotonated form has been reported for a black dye by Nazeeruddin et al.; the absorption bands of the black dye are blue-shifted as the pH of the solution increased,⁷ i.e., by increasing the ratio of the deprotonated form. Moreover, Hara et al. have reported that the blue shift in the deprotonated form of the dyes was observed in going from a methanol solution to a TiO_2 surface.⁴

IV. Summary

Using TD-DFT, CIS, and CC2, we investigate the absorption spectra of C343, NKX-2388, NKX-2311, NKX-2586, and NKX-2677 coumarin dyes, which are useful candidates for use in

efficient dye-sensitized solar cells (DSSC). To analyze the solvent and deprotonation effects, three different chemical environments are considered. The solvent effects are taken into account by the PCM. The CC2 calculation shows good agreement with the experimental results except for C343. TD-DFT underestimates the vertical excitation energy of NKX-2586 and -2677. The methanol solution is found to induce a red shift in the vertical excitation energy due to the stabilization of the LUMO (π^* orbital). In the deprotonated form, a blue shift is observed due to the destabilization of the LUMO. We expect that the theoretical investigation of the excited-state properties for these coumarin dyes will help to design more efficient functional molecules.

Acknowledgment. This research was supported in part by a Grant-in-Aid for Scientific Research in Specially Promoted Research “Simulations and Dynamics for Real Systems” and a grant for the 21st Century COE Program “Human-Friendly Materials based on Chemistry” from the Ministry of Education, Science, Culture, and Sports, Japan. This research was also partly supported by the Core Research for Evolutional Science and Technology (CREST) Program, “High Performance Computing for Multi-Scale and Multi-Physics Phenomena” of the Japan Science and Technology Agency (JST). We thank Dr. M. A. Watson and Dr. K. Yagi for useful suggestions on the manuscript. Y.K. is supported by the Japan Society for the Promotion of Science (JSPS) Research Fellowship for Young Scientist.

References and Notes

- (1) O'Regan, B.; Grätzel, M. *Nature* **1991**, *353*, 737.
- (2) Hara, K.; Sato, T.; Katoh, R.; Furube, A.; Ohge, Y.; Shinpo, A.; Suga, S.; Sayama, K.; Sugihara, H.; Arakawa, H. *J. Phys. Chem. B* **2003**, *107*, 597–606.
- (3) Hara, K.; Kurashige, M.; Dan-oh, Y.; Kasada, C.; Shinpo, A.; Suga, S.; Sayama, K.; Arakawa, H. *New. J. Chem.* **2003**, *27*, 783.
- (4) Hara, K.; Wang, Z.-S.; Sato, T.; Furube, A.; Katoh, R.; Sugihara, H.; Dan-oh, Y.; Kasada, C.; Shinpo, A. *J. Phys. Chem. B* **2005**, *109*, 15476.
- (5) Barbe, C. J.; Arendse, F.; Comte, P.; Jirousek, M.; Lenzmann, F.; Shklover, V.; Grätzel, M. *J. Am. Cer. Soc.* **1997**, *80*, 3157.
- (6) Grätzel, M. *Catech* **1999**, *3*, 4.
- (7) Nazeeruddin, M. K.; Péchy, P.; Renouard, T.; Zakeeruddin, S. M.; Humphry-Baker, R.; Comte, P.; Liska, P.; Cevey, L.; Costa, E.; Shklover, V.; Spiccia, L.; Deacon, G. B.; Bigonozzi, C. A.; Grätzel, M. *J. Am. Chem. Soc.* **2001**, *123*, 1613.
- (8) Cave, R. J.; Burke, K.; Caster, E. W., Jr. *J. Phys. Chem. A* **2002**, *106*, 9294.
- (9) Cave, R. J.; Caster, E. W., Jr. *J. Phys. Chem. A* **2002**, *106*, 12117.
- (10) Georgieva, I.; Trendafilova, N.; Aquino, A.; Lischka, H. *J. Phys. Chem. A* **2005**, *109*, 11860.
- (11) Jacquemin, D.; Perpète, E. A.; Scalmani, G.; Frisch, M. J.; Assfeld, X.; Ciofini, I.; Adamo, C. *J. Chem. Phys.* **2006**, *125*, 164324.
- (12) Improta, R.; Barone, V.; Santoro, F. *Angew. Int. Ed.* **2007**, *46*, 405.
- (13) Santoro, F.; Improta, R.; Lami, A.; Bloino, J.; Barone, V. *J. Chem. Phys.* **2007**, *126*, 084509.
- (14) Preat, J.; Jacquemin, D.; Wathelet, V.; André, J.-M.; Perpète, E. A. *J. Phys. Chem. A* **2006**, *110*, 8144.
- (15) Improta, R.; Barone, V.; Scalmani, G.; Frisch, M. J. *J. Chem. Phys.* **2006**, *125*, 054103.
- (16) Preat, J.; Jacquemin, D.; Perpète, E. A. *Chem. Phys. Lett.* **2005**, *415*, 20.
- (17) Runge, E.; Gross, E. K. U. *Phys. Rev. Lett.* **1984**, *52*, 997.
- (18) Christiansen, O.; Koch, H.; Jørgensen, P. *Chem. Phys. Lett.* **1995**, *243*, 409.
- (19) Hättig, C. *J. Chem. Phys.* **2003**, *118*, 7751.
- (20) Köhn, A.; Hättig, C. *J. Chem. Phys.* **2003**, *119*, 5021.
- (21) Tomasi, J.; Persico, M. *Chem. Rev.* **1994**, *94*, 2027.
- (22) Hehre, W. J.; Ditchfield, R.; Pople, J. A. *J. Chem. Phys.* **1972**, *56*, 2257.
- (23) Hariharan, P. C.; Pople, J. A. *Theor. Chim. Acta* **1973**, *28*, 213.
- (24) Francl, M. M.; Pietro, W. J.; Hehre, W. J.; Binkley, J. S.; Gordon, M. S.; DeFrees, D. J.; Pople, J. A. *J. Chem. Phys.* **1982**, *77*, 3654.
- (25) Clark, T.; Chandrasekhar, J.; Schleyer, P. V. R. *J. Comput. Chem.* **1983**, *4*, 294.

- (26) Schäfer, A.; Horn, H.; Ahlrichs, R. *J. Chem. Phys.* **1992**, *97*, 2571.
- (27) Weigend, F.; Häser, M.; Patzelt, H.; Ahlrichs, R. *Chem. Phys. Lett.* **1998**, *294*, 143.
- (28) Cossi, M.; Barone, V. *J. Chem. Phys.* **2001**, *115*, 4708.
- (29) Frisch, M. J.; Trucks, G. W.; Schlegel, H. B.; Scuseria, G. E.; Robb, M. A.; Cheeseman, J. R.; Montgomery, J. A., Jr.; Vreven, T.; Kudin, K. N.; Burant, J. C.; Millam, J. M.; Iyengar, S. S.; Tomasi, J.; Barone, V.; Mennucci, B.; Cossi, M.; Scalmani, G.; Rega, N.; Petersson, G. A.; Nakatsuji, H.; Hada, M.; Ehara, M.; Toyota, K.; Fukuda, R.; Hasegawa, J.; Ishida, M.; Nakajima, T.; Honda, Y.; Kitao, O.; Nakai, H.; Klene, M.; Li, X.; Knox, J. E.; Hratchian, H. P.; Cross, J. B.; Bakken, V.; Adamo, C.; Jaramillo, J.; Gomperts, R.; Stratmann, R. E.; Yazyev, O.; Austin, A. J.; Cammi, R.; Pomelli, C.; Ochterski, J. W.; Ayala, P. Y.; Morokuma, K.; Voth, G. A.; Salvador, P.; Dannenberg, J. J.; Zakrzewski, V. G.; Dapprich, S.; Daniels, A. D.; Strain, M. C.; Farkas, O.; Malick, D. K.; Rabuck, A. D.; Raghavachari, K.; Foresman, J. B.; Ortiz, J. V.; Cui, Q.; Baboul, A. G.; Clifford, S.; Cioslowski, J.; Stefanov, B. B.; Liu, G.; Liashenko, A.; Piskorz, P.; Komaromi, I.; Martin, R. L.; Fox, D. J.; Keith, T.; Al-Laham, M. A.; Peng, C. Y.; Nanayakkara, A.; Challacombe, M.; Gill, P. M. W.; Johnson, B.; Chen, W.; Wong, M. W.; Gonzalez, C.; Pople, J. A. *Gaussian 03*, revision C.02; Gaussian, Inc.: Wallingford, CT, 2004.
- (30) Ahlrichs, R.; Bär, M.; Häser, M.; Horn, M. H.; Kölmel, C. *Chem. Phys. Lett.* **1989**, *162*, 165.